

Observation of $B^{\mp} \rightarrow \rho^{\mp} \rho^0$ Decays

J. Zhang,⁴⁸ M. Nakao,⁸ K. Abe,⁸ K. Abe,⁴¹ T. Abe,⁴² I. Adachi,⁸ H. Aihara,⁴³ M. Akatsu,²² Y. Asano,⁴⁸ T. Aso,⁴⁷ V. Aulchenko,² T. Aushev,¹² S. Bahinipati,⁵ A. M. Bakich,³⁸ Y. Ban,³³ E. Banas,²⁷ P. K. Behera,⁴⁹ I. Bizjak,¹³ A. Bondar,² A. Bozek,²⁷ M. Bračko,^{20,13} T. E. Browder,⁷ B. C. K. Casey,⁷ P. Chang,²⁶ Y. Chao,²⁶ B. G. Cheon,³⁷ R. Chistov,¹² S.-K. Choi,⁶ Y. Choi,³⁷ Y. K. Choi,³⁷ M. Danilov,¹² L. Y. Dong,¹⁰ J. Dragic,²¹ A. Drutskoy,¹² S. Eidelman,² V. Eiges,¹² Y. Enari,²² C. Fukunaga,⁴⁵ N. Gabyshev,⁸ A. Garmash,^{2,8} T. Gershon,⁸ A. Gordon,²¹ R. Guo,²⁴ F. Handa,⁴² T. Hara,³¹ N. C. Hastings,⁸ H. Hayashii,²³ M. Hazumi,⁸ L. Hinz,¹⁸ T. Hokuue,²² Y. Hoshi,⁴¹ W.-S. Hou,²⁶ Y. B. Hsiung,^{26,*} H.-C. Huang,²⁶ Y. Igarashi,⁸ T. Iijima,²² K. Inami,²² A. Ishikawa,²² R. Itoh,⁸ H. Iwasaki,⁸ M. Iwasaki,⁴³ Y. Iwasaki,⁸ H. K. Jang,³⁶ J. H. Kang,⁵² J. S. Kang,¹⁵ S. U. Kataoka,²³ N. Katayama,⁸ H. Kawai,³ N. Kawamura,¹ T. Kawasaki,²⁹ D. W. Kim,³⁷ H. J. Kim,⁵² Hyunwoo Kim,¹⁵ J. H. Kim,³⁷ S. K. Kim,³⁶ K. Kinoshita,⁵ P. Koppenburg,⁸ S. Korpar,^{20,13} P. Križan,^{19,13} P. Krokovny,² R. Kulasiri,⁵ S. Kumar,³² A. Kuzmin,² Y.-J. Kwon,⁵² G. Leder,¹¹ S. H. Lee,³⁶ T. Lesiak,²⁷ J. Li,³⁵ A. Limosani,²¹ S.-W. Lin,²⁶ D. Liventsev,¹² J. MacNaughton,¹¹ G. Majumder,³⁹ F. Mandl,¹¹ D. Marlow,³⁴ H. Matsumoto,²⁹ T. Matsumoto,⁴⁵ A. Matyja,²⁷ W. Mitaroff,¹¹ K. Miyabayashi,²³ H. Miyata,²⁹ D. Mohapatra,⁵⁰ T. Mori,⁴ T. Nagamine,⁴² Y. Nagasaka,⁹ T. Nakadaira,⁴³ E. Nakano,³⁰ J. W. Nam,³⁷ Z. Natkaniec,²⁷ S. Nishida,¹⁶ O. Nitoh,⁴⁶ T. Nozaki,⁸ S. Ogawa,⁴⁰ T. Ohshima,²² T. Okabe,²² S. Okuno,¹⁴ S. L. Olsen,⁷ W. Ostrowicz,²⁷ H. Ozaki,⁸ H. Park,¹⁷ K. S. Park,³⁷ N. Parslow,³⁸ J.-P. Perroud,¹⁸ L. E. Piilonen,⁵⁰ M. Rozanska,²⁷ H. Sagawa,⁸ S. Saitoh,⁸ Y. Sakai,⁸ T. R. Sarangi,⁴⁹ A. Satpathy,^{8,5} O. Schneider,¹⁸ J. Schümann,²⁶ C. Schwanda,^{8,11} A. J. Schwartz,⁵ S. Semenov,¹² K. Senyo,²² R. Seuster,⁷ M. E. Sevier,²¹ T. Shibata,²⁹ H. Shibuya,⁴⁰ V. Sidorov,² J. B. Singh,³² S. Stanič,^{8,†} M. Starič,¹³ A. Sugi,²² K. Sumisawa,⁸ T. Sumiyoshi,⁴⁵ S. Suzuki,⁵¹ S. Y. Suzuki,⁸ S. K. Swain,⁷ T. Takahashi,³⁰ F. Takasaki,⁸ K. Tamai,⁸ N. Tamura,²⁹ M. Tanaka,⁸ G. N. Taylor,²¹ Y. Teramoto,³⁰ T. Tomura,⁴³ S. N. Tovey,²¹ K. Trabelsi,⁷ T. Tsuboyama,⁸ T. Tsukamoto,⁸ S. Uehara,⁸ S. Uno,⁸ G. Varner,⁷ K. E. Varvell,³⁸ C. C. Wang,²⁶ C. H. Wang,²⁵ J. G. Wang,⁵⁰ M.-Z. Wang,²⁶ Y. Watanabe,⁴⁴ E. Won,¹⁵ B. D. Yabsley,⁵⁰ Y. Yamada,⁸ A. Yamaguchi,⁴² Y. Yamashita,²⁸ M. Yamauchi,⁸ H. Yanai,²⁹ Heyoung Yang,³⁶ Y. Yusa,⁴² Z. P. Zhang,³⁵ Y. Zheng,⁷ V. Zhilich,² D. Žontar,^{19,13} and D. Zürcher¹⁸

(The Belle Collaboration)

¹Aomori University, Aomori

²Budker Institute of Nuclear Physics, Novosibirsk

³Chiba University, Chiba

⁴Chuo University, Tokyo

⁵University of Cincinnati, Cincinnati, Ohio 45221

⁶Gyeongsang National University, Chinju

⁷University of Hawaii, Honolulu, Hawaii 96822

⁸High Energy Accelerator Research Organization (KEK), Tsukuba

⁹Hiroshima Institute of Technology, Hiroshima

¹⁰Institute of High Energy Physics, Chinese Academy of Sciences, Beijing

¹¹Institute of High Energy Physics, Vienna

¹²Institute for Theoretical and Experimental Physics, Moscow

¹³J. Stefan Institute, Ljubljana

¹⁴Kanagawa University, Yokohama

¹⁵Korea University, Seoul

¹⁶Kyoto University, Kyoto

¹⁷Kyungpook National University, Taegu

¹⁸Institut de Physique des Hautes Énergies, Université de Lausanne, Lausanne

¹⁹University of Ljubljana, Ljubljana

²⁰University of Maribor, Maribor

²¹University of Melbourne, Victoria

²²Nagoya University, Nagoya

²³Nara Women's University, Nara

²⁴National Kaohsiung Normal University, Kaohsiung

²⁵National Lien-Ho Institute of Technology, Miao Li

²⁶Department of Physics, National Taiwan University, Taipei

²⁷H. Niewodniczanski Institute of Nuclear Physics, Krakow

²⁸Nihon Dental College, Niigata

²⁹Niigata University, Niigata

- ³⁰Osaka City University, Osaka
³¹Osaka University, Osaka
³²Panjab University, Chandigarh
³³Peking University, Beijing
³⁴Princeton University, Princeton, New Jersey 08545
³⁵University of Science and Technology of China, Hefei
³⁶Seoul National University, Seoul
³⁷Sungkyunkwan University, Suwon
³⁸University of Sydney, Sydney, NSW
³⁹Tata Institute of Fundamental Research, Bombay
⁴⁰Toho University, Funabashi
⁴¹Tohoku Gakuin University, Tagajo
⁴²Tohoku University, Sendai
⁴³Department of Physics, University of Tokyo, Tokyo
⁴⁴Tokyo Institute of Technology, Tokyo
⁴⁵Tokyo Metropolitan University, Tokyo
⁴⁶Tokyo University of Agriculture and Technology, Tokyo
⁴⁷Toyama National College of Maritime Technology, Toyama
⁴⁸University of Tsukuba, Tsukuba
⁴⁹Utkal University, Bhubaneswer
⁵⁰Virginia Polytechnic Institute and State University, Blacksburg, Virginia 24061
⁵¹Yokkaichi University, Yokkaichi
⁵²Yonsei University, Seoul

(Received 3 June 2003; published 24 November 2003)

We report the first observation of the charmless vector-vector decay process $B^\mp \rightarrow \rho^\mp \rho^0$. The measurement uses a 78 fb^{-1} data sample collected with the Belle detector at the KEKB asymmetric e^+e^- collider operating at the $\Upsilon(4S)$ resonance. We obtain a branching fraction of $\mathcal{B}(B^\mp \rightarrow \rho^\mp \rho^0) = [31.7 \pm 7.1(\text{stat})_{-6.7}^{+3.8}(\text{syst})] \times 10^{-6}$. An analysis of the ρ helicity-angle distributions gives a longitudinal polarization fraction of $\Gamma_L/\Gamma = 0.95 \pm 0.11(\text{stat}) \pm 0.02(\text{syst})$. We also measure the direct- CP -violating asymmetry $\mathcal{A}_{CP}(B^\mp \rightarrow \rho^\mp \rho^0) = 0.00 \pm 0.22(\text{stat}) \pm 0.03(\text{syst})$.

DOI: 10.1103/PhysRevLett.91.221801

PACS numbers: 13.25.Hw, 14.40.Nd

Charmless B meson decays to two pseudoscalar mesons or to pseudoscalar plus vector meson final states have been studied in some detail [1]. However, measurements of decays to charmless vector-vector (VV) final states are rather limited; to date, only $B \rightarrow \phi K^*$ decays have been observed [2]. The VV decays provide opportunities to search for direct- CP and/or T violation through angular correlations between the vector meson decay final states [3,4]. The decay $B^\mp \rightarrow \rho^\mp \rho^0$ is a tree-dominated $b \rightarrow u$ process and can be used in an isospin analysis [5] to extract the Cabibbo-Kobayashi-Maskawa angle ϕ_2 from $B \rightarrow \rho\rho$ decays. In these decays isospin-breaking processes such as electroweak penguins [6] or ρ^0 - ω interference [7,8], which may produce a sizable direct- CP -violating asymmetry (\mathcal{A}_{CP}), are expected to be enhanced relative to CP -conserving processes such as gluonic penguins, which are nominally forbidden by isospin symmetry. The branching fraction for this process is predicted to be $\mathcal{O}(10^{-5})$ [8,9].

In this Letter, we present the first observation of the VV decay mode $B^\mp \rightarrow \rho^\mp \rho^0$. (The inclusion of charge conjugate modes is implied unless stated otherwise.) These decays produce final states where both ρ mesons are either longitudinally or transversely polarized.

The analysis is based on a 78 fb^{-1} data sample containing 85×10^6 B meson pairs collected at the $\Upsilon(4S)$

resonance with the Belle detector at the KEKB asymmetric-energy e^+e^- (3.5 and 8.0 GeV) collider. We also use an off-resonance data sample of 8.3 fb^{-1} collected at a center-of-mass energy that is 60 MeV below the $\Upsilon(4S)$ resonance.

The Belle detector is a large-solid-angle magnetic spectrometer. Charged particle tracking is provided by a three-layer silicon vertex detector and a 50-layer central drift chamber (CDC). Charged hadron identification is provided by dE/dx measurements in the CDC and arrays of aerogel threshold Čerenkov counters (ACC) and time-of-flight scintillation counters (TOF) that surround the CDC. An electromagnetic calorimeter comprised of CsI(Tl) crystals (ECL) provides photon detection and electron identification. All of these devices are located inside a superconducting solenoidal coil that provides a 1.5 T magnetic field. An iron flux return located outside of the coil is instrumented to detect K_L^0 mesons and muons. The detector is described in detail elsewhere [10].

We select $B^\mp \rightarrow \rho^\mp \rho^0$ candidate events by combining three charged pions and one neutral pion. We require that each charged track has a transverse momentum $p_t > 0.1 \text{ GeV}/c$ and is consistent with originating from within $\delta r < 0.1 \text{ cm}$ in the radial direction and $|\delta z| < 5 \text{ cm}$ in the electron beam direction of the run-by-run-determined interaction point. We also require that the three charged

tracks be positively identified as pions by the CDC, ACC, and TOF systems.

Candidate π^0 mesons are reconstructed from pairs of photons with an invariant mass in the range $0.118 \text{ GeV}/c^2 < M(\gamma\gamma) < 0.150 \text{ GeV}/c^2$. On average, this corresponds to a $\pm 3\sigma$ requirement. For the ECL barrel region ($32.2^\circ < \theta < 128.7^\circ$), photon energies greater than 50 MeV are required; for the ECL end-cap region ($17.0^\circ < \theta < 31.4^\circ$ or $130.7^\circ < \theta < 150.0^\circ$), this requirement is increased to 100 MeV. In addition, we accept only π^0 candidates with a $Y(4S)$ center-of-mass system (c.m.s.) momentum $p_{\pi^0} > 0.5 \text{ GeV}/c$. The π^0 candidates are kinematically constrained to the nominal π^0 mass. Candidate ρ mesons are reconstructed via their $\rho^0 \rightarrow \pi^+\pi^-$ and $\rho^+ \rightarrow \pi^+\pi^0$ decays. For both the charged and neutral modes, we require $0.65 \text{ GeV}/c^2 < M(\pi\pi) < 0.89 \text{ GeV}/c^2$.

$B^+ \rightarrow \rho^+\rho^0$ decays are identified using the beam-energy constrained mass $M_{bc} \equiv \sqrt{(E_{\text{beam}})^2 - (p_B)^2}$ and the energy difference $\Delta E \equiv E_B - E_{\text{beam}}$, where E_{beam} is the c.m.s. beam energy, and p_B and E_B are the c.m.s. momentum and energy, respectively, of the $B^+ \rightarrow \rho^+\rho^0$ candidates. The ΔE distribution has a tail on the lower side caused by incomplete longitudinal containment of electromagnetic showers in the CsI crystals, and the ΔE resolution varies slightly depending on the π^0 momentum. We select events in the region $|\Delta E| < 0.4 \text{ GeV}$, $M_{bc} > 5.2 \text{ GeV}/c^2$, with a signal region defined as $-0.10 \text{ GeV} < \Delta E < 0.06 \text{ GeV}$ and $5.272 \text{ GeV}/c^2 < M_{bc} < 5.290 \text{ GeV}/c^2$. These requirements correspond to approximately $\pm 3\sigma$ for both quantities.

In the longitudinally polarized H_{00} state, one of the $\rho \rightarrow \pi\pi$ daughters has low momentum (0–1.3 GeV/c) while the other has high momentum (1.3–2.8 GeV/c); in the transversely polarized H_{11} state, the two pions tend to have the same momentum. Thus, the H_{00} state has a lower reconstruction efficiency and a ΔE resolution that is, on average, about 15% broader than that for the H_{11} state.

There are large backgrounds from $e^+e^- \rightarrow q\bar{q}$ continuum events ($q = u, d, s, c$), which tend to have a two-jet-like structure. These are suppressed by requiring $|\cos\theta_{\text{thr}}| < 0.8$, where θ_{thr} is the angle between the thrust axis of the candidate tracks plus neutrals and that of the remaining tracks in the event. We achieve further suppression by a likelihood ratio requirement derived from a Fisher discriminant formed from six modified Fox-Wolfram moments [11] and θ_B , the angle between the B flight direction and the electron beam direction. The combined rejection for continuum events is 98%, with a 65% loss in signal.

Background contributions from $b \rightarrow c$ processes are investigated with a large sample of Monte Carlo (MC) events, for which no signal-like peak is found in either the ΔE or M_{bc} distributions. Some rare B decay processes, such as $B^+ \rightarrow \eta'\rho^+$, $K^{*+}\rho^0$, ρ^+K^{*0} , and $\rho\pi$, can survive the event selection but are displaced from the signal in

ΔE . Moreover, these modes have small branching fractions [12] and low reconstruction efficiencies. MC estimates based on measured upper limits for the branching fractions indicate a possible signal-region yield from these rare modes of seven events; this is taken into account in the systematic error determination, as discussed below, but these rare B decay processes are not included in the MC plotted in the following figures.

Figure 1 (left) shows the ΔE projection of the selected entries in the $5.272 \text{ GeV}/c^2 < M_{bc} < 5.290 \text{ GeV}/c^2$ signal region. The curve shows the results of a binned maximum-likelihood fit with three components: signal, continuum background, and $B\bar{B}$ background. The signal is represented by the sum of a Gaussian and a ‘‘crystal ball’’ line shape function [13] with parameters determined from an H_{00} signal MC that is calibrated with $B^+ \rightarrow \bar{D}^0\pi^+$, $\bar{D}^0 \rightarrow K^+\pi^-\pi^0$ events. A linear function with a slope determined from the off-resonance data is used to represent the continuum background. The $B\bar{B}$ background contribution is modeled by a smoothed histogram with a shape that is obtained from MC. In the fit, all parameters other than the three normalizations are fixed.

The fit gives a signal yield of 59 ± 13 entries. The statistical significance of the signal, defined as $\sqrt{-2\ln(\mathcal{L}_0/\mathcal{L}_{\text{max}})}$, where \mathcal{L}_{max} is the likelihood value at the best-fit signal yield and \mathcal{L}_0 is the value with the signal yield fixed to zero, is 5.3.

Figure 1 (right) shows the M_{bc} projection of entries in the $-0.10 \text{ GeV} < \Delta E < 0.06 \text{ GeV}$ signal region. The curve shows the results of a binned maximum-likelihood fit that uses a single Gaussian with a MC-determined width to represent the signal, a threshold (ARGUS) function [14] for the continuum background with shape parameters that are determined from the ΔE sideband (defined as $0.1 \text{ GeV} < \Delta E < 0.4 \text{ GeV}$), and a smoothed histogram obtained from MC to represent the $B\bar{B}$ background, normalized according to the MC expectation. This three-parameter fit gives a signal yield of 49 ± 10 entries, with a statistical significance of 6.5. The fit results are summarized in Table I.

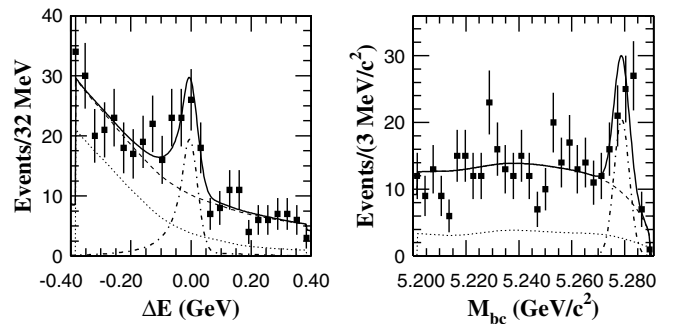


FIG. 1. ΔE (left) and M_{bc} (right) fits to the $B^+ \rightarrow \rho^+\rho^0$ candidates (see text). The signal component is shown as a dot-dashed line. The sum of $B\bar{B}$ and continuum components is shown as a dashed line. The dotted lines represent the $B\bar{B}$ background.

TABLE I. Signal yields from the fits to the ΔE and M_{bc} distributions together with the MC-determined efficiencies: ϵ_{00} for the H_{00} state and ϵ_{11} for the H_{11} state.

	ΔE fit	M_{bc} fit
Yield	59 ± 13 (5.3 σ)	49 ± 10 (6.5 σ)
Efficiency ϵ_{00}	2.11%	1.59%
Efficiency ϵ_{11}	3.45%	3.07%

Figure 2 shows signal yields extracted from fits to the ΔE distributions for different $M(\pi^+\pi^-)$ and $M(\pi^+\pi^0)$ mass bins; the $\pi\pi$ mass spectra from the signal MC are shown as histograms. The data agree reasonably well with $B^+ \rightarrow \rho^+\rho^0$ MC expectations.

We examined the possible contribution from nonresonant processes using MC-generated $B^+ \rightarrow \pi^+\pi^-\pi^+\pi^0$ events where the final states are distributed uniformly over phase space. After the application of all selection requirements, including the ρ mass cuts, we find an efficiency that is less than 2% of that for $B^+ \rightarrow \rho^+\rho^0$ decays. Possible contributions from $B^+ \rightarrow a_1^+\pi^0$ or $B^+ \rightarrow a_1^0\pi^+$ decay are examined and found to be smaller than those from nonresonant decays. To account for these contributions, we perform χ^2 fits to the distributions shown in Fig. 2 with a ρ plus nonresonant $\pi\pi$ component included. The resulting nonresonant yield increased by 1σ is included in the systematic error.

We use the $\rho \rightarrow \pi\pi$ helicity-angle (θ_{hel}) distributions to determine the relative strengths of H_{00} and H_{11} . Here θ_{hel} is the angle between an axis antiparallel to the B flight direction and the π^+ flight direction in the ρ rest frame. For the H_{00} state, the distribution in θ_{hel} is proportional to $\cos^2\theta_{\text{hel}(\rho 0)}\cos^2\theta_{\text{hel}(\rho +)}$, and for the H_{11} state the distribution is $\sin^2\theta_{\text{hel}(\rho 0)}\sin^2\theta_{\text{hel}(\rho +)}$, where $\theta_{\text{hel}(\rho 0)}$ ($\theta_{\text{hel}(\rho +)}$) is the helicity angle for ρ^0 (ρ^+). The signal yields determined from fits to the ΔE distributions for each helicity-angle bin are plotted versus $\cos\theta_{\text{hel}}$ in Fig. 3 for the ρ^0 (left) and the ρ^+ (right). We fit the yields using a ΔE signal width that depends on $\cos\theta_{\text{hel}(\rho +)}$ and determined from an H_{00} signal MC. We perform a simultaneous χ^2 fit to the two background-subtracted ρ helicity-angle distributions using MC-determined expectations for the H_{00} and H_{11} helicity states. The fit results, shown as histograms in Fig. 3, give 48 ± 11 longitudinally polarized and 4 ± 9 transversely polarized events; this indicates that the longitudinal (H_{00}) state dominates. We obtain the acceptance-corrected longitudinal polarization fraction

$$\Gamma_L/\Gamma = 0.95 \pm 0.11(\text{stat}) \pm 0.02(\text{syst}),$$

where the systematic error includes uncertainties in the signal yield extraction and the polarization dependence of the detection efficiency. This dominance of H_{00} is consistent with theoretical predictions [15].

Since the ΔE distribution provides stronger discrimination against rare B -meson decay backgrounds, we use

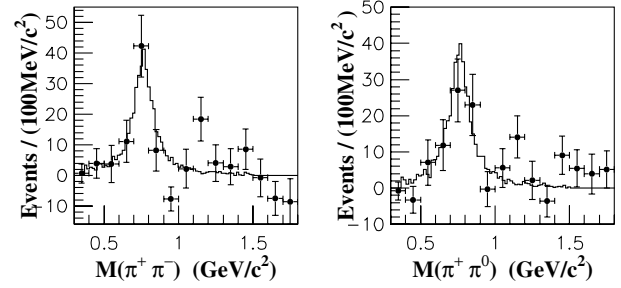


FIG. 2. Data points are the results of fits to the ΔE distributions for each $M(\pi^+\pi^-)$ bin (left) and $M(\pi^+\pi^0)$ bin (right), where the histograms are expectations from the signal MC.

the ΔE fit result and MC-determined efficiencies weighted by the measured polarization components to calculate the branching fraction. In the calculation, the production rates of B^+B^- and $B^0\bar{B}^0$ pairs are assumed to be equal. We assign a 3.4% systematic error for the uncertainty in track-finding efficiency that is obtained from a study of partially reconstructed D^* decays; a 3.6% error for the particle identification efficiency that is based on a study of kinematically selected $D^{*+} \rightarrow D^0\pi^+$, $D^0 \rightarrow K^-\pi^+$ decays; a 4.0% systematic error for the uncertainty in the π^0 detection efficiency that is determined from data-MC comparisons of $\eta \rightarrow \pi^0\pi^0\pi^0$ to $\eta \rightarrow \pi^+\pi^-\pi^0$ and $\eta \rightarrow \gamma\gamma$, also checked with inclusive high momentum D^0 's from the continuum tagged via $D^* \rightarrow D^0\pi$, and look at $D^0 \rightarrow K\pi\pi^0$ decays; a 5.4% error for continuum suppression that is estimated from a study of $B^+ \rightarrow \bar{D}^0\pi^+$, $\bar{D}^0 \rightarrow K^+\pi^-\pi^0$ decays; an error associated with the ΔE fit of ${}_{-6.7}^{+7.3}\%$ that is obtained from changes that occur when each parameter of the fitting functions is varied by $\pm 1\sigma$; a 1% error for the uncertainty in the number of $B\bar{B}$ events in the data sample; a ${}_{-16.7}^{+0}\%$ error to account for a possible contribution from nonresonant decays; and a 3.3% error due to uncertainties in the rare B decay background that is estimated from the change produced by fitting the ΔE

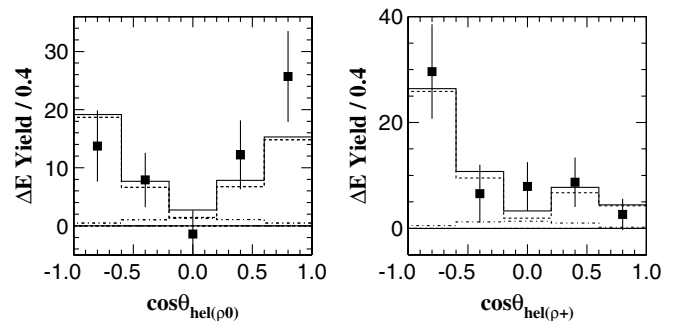


FIG. 3. Data points show the background-subtracted $\cos\theta_{\text{hel}}$ distributions for the ρ^0 (left) and ρ^+ (right). In each plot the dashed (dot-dashed) histogram is the H_{00} (H_{11}) component of the fit; the solid histogram is their sum. The low yield of events near $\cos\theta_{\text{hel}(\rho^+)} = 1$ is due to the $p_{\pi^0} > 0.5$ GeV/ c requirement.

distribution with the inclusion of an additional component normalized at its MC expectation. We also include a ${}_{-6.5}^{+3.1}\%$ error due to the uncertainty in the fraction of longitudinal polarization. The quadratic sum of all of these errors is taken as the total systematic error. We obtain the branching fraction

$$\mathcal{B}(B^+ \rightarrow \rho^+ \rho^0) = [31.7 \pm 7.1(\text{stat})_{-6.7}^{+3.8}(\text{syst})] \times 10^{-6}.$$

As a check, we examined the decay mode $B^+ \rightarrow \rho^+ \bar{D}^0$, $\bar{D}^0 \rightarrow \pi^+ \pi^-$, which has the same final state particles as the mode under study, including a π^0 with a similar momentum distribution. The same analysis procedure is applied except for an $|M(\pi\pi) - M_{D^0}| < 13 \text{ MeV}/c^2$ mass selection. For this mode, we obtain a signal yield of 42 ± 8 events, consistent with MC expectations based on the known branching fraction values [1].

Direct CP violation would be indicated by a difference in partial rates for $B^- \rightarrow \rho^- \rho^0$ and $B^+ \rightarrow \rho^+ \rho^0$. Separate fits to the ΔE distributions find $29 \pm 9 \rho^- \rho^0$ and $29 \pm 9 \rho^+ \rho^0$ events. Since backgrounds from generic $B\bar{B}$ decays should contribute equally to $\rho^- \rho^0$ and $\rho^+ \rho^0$, we fix the normalizations for $B\bar{B}$ components at half the value determined from the combined fit.

The charge symmetry of the detector and reconstruction procedure is verified with a sample of $B^+ \rightarrow \bar{D}^0 \pi^+$, $\bar{D}^0 \rightarrow K^+ \pi^- \pi^0$ decays and their charge conjugates. Here the analysis procedure is similar to that for $B^+ \rightarrow \rho^+ \rho^0$ but replaces one π^+ by a K^+ and uses the invariant mass requirement $|M(K\pi\pi^0) - M_{D^0}| < 50 \text{ MeV}/c^2$. For these events we find a direct- CP -violating asymmetry of $(-2.1 \pm 2.5)\%$, which is consistent with zero. We assign 2.5% as the systematic error for the detection and reconstruction asymmetry. The systematic error associated with the ΔE fitting procedure is determined to be $(+0.8 - 1.2)\%$ by shifting each parameter of the fitting functions by $\pm 1\sigma$ and taking the quadratic sum of the resulting changes in \mathcal{A}_{CP} . The quadratic sum of these errors is taken as the total systematic error. We obtain the CP asymmetry

$$\begin{aligned} \mathcal{A}_{CP}(B^\mp \rightarrow \rho^\mp \rho^0) &\equiv \frac{N_{(\rho^- \rho^0)} - N_{(\rho^+ \rho^0)}}{N_{(\rho^- \rho^0)} + N_{(\rho^+ \rho^0)}} \\ &= 0.00 \pm 0.22(\text{stat}) \pm 0.03(\text{syst}). \end{aligned}$$

In summary, we have observed the decay $B^\mp \rightarrow \rho^\mp \rho^0$ with a statistical significance of a combined maximum likelihood fit of 5.3σ . We measure the branching fraction to be $\mathcal{B}(B^\mp \rightarrow \rho^\mp \rho^0) = [31.7 \pm 7.1(\text{stat})_{-6.7}^{+3.8}(\text{syst})] \times 10^{-6}$, where the systematic error includes the error associated with the helicity-mix uncertainty. An analysis of the helicity-angle distributions gives the longitudinal polarization fraction $\Gamma_L/\Gamma = 0.95 \pm 0.11(\text{stat}) \pm 0.02(\text{syst})$. We also measure the direct- CP -violating

asymmetry $\mathcal{A}_{CP}(B^\mp \rightarrow \rho^\mp \rho^0) = 0.00 \pm 0.22(\text{stat}) \pm 0.03(\text{syst})$.

We thank the KEKB accelerator group for the excellent operation of the KEKB accelerator. We acknowledge support from the Ministry of Education, Culture, Sports, Science, and Technology of Japan and the Japan Society for the Promotion of Science; the Australian Research Council and the Australian Department of Industry, Science and Resources; National Science Foundation of China under Contract No. 10175071; the Department of Science and Technology of India; the BK21 program of the Ministry of Education of Korea and the CHEP SRC program of the Korea Science and Engineering Foundation; the Polish State Committee for Scientific Research under Contract No. 2P03B 01324; the Ministry of Science and Technology of Russian Federation; the Ministry of Education, Science and Sport of Slovenia; the National Science Council and the Ministry of Education of Taiwan; and the U.S. Department of Energy.

*On leave from Fermi National Accelerator Laboratory, Batavia, Illinois 60510.

†On leave from Nova Gorica Polytechnic, Nova Gorica.

- [1] K. Hagiwara *et al.*, Phys. Rev. D **66**, 010001 (2002).
- [2] CLEO Collaboration, R. A. Briere *et al.*, Phys. Rev. Lett. **86**, 3718 (2001); BABAR Collaboration, B. Aubert *et al.*, Phys. Rev. Lett. **87**, 151801 (2001).
- [3] G. Kramer, W.F. Palmer, and H. Simma, Nucl. Phys. **B428**, 77 (1994).
- [4] A. Datta and D. London, hep-ph/0303159.
- [5] M. Gronau and D. London, Phys. Rev. Lett. **65**, 3381 (1990); Y. Grossman and H. Quinn, Phys. Rev. D **58**, 017504 (1998).
- [6] D. Atwood and A. Soni, Phys. Rev. D **65**, 073018 (2002).
- [7] S. Gardner, H. B. O'Connell, and A.W. Thomas, Phys. Rev. Lett. **80**, 1834 (1998).
- [8] R. Enomoto and M. Tanabashi, Phys. Lett. B **386**, 413 (1996).
- [9] W.S. Hou and K.C. Yang, Phys. Rev. D **61**, 073014 (2000).
- [10] Belle Collaboration, A. Abashian *et al.*, Nucl. Instrum. Methods Phys. Res., Sect. A **479**, 117 (2002).
- [11] G.C. Fox and S. Wolfram, Phys. Lett. B **41**, 1581 (1978); Belle Collaboration, K. Abe *et al.*, Phys. Rev. Lett. **87**, 101801 (2001).
- [12] CLEO Collaboration, C.P. Jessop *et al.*, Phys. Rev. Lett. **85**, 2881 (2000); CLEO Collaboration, R. Godang *et al.*, Phys. Rev. Lett. **88**, 021802 (2002).
- [13] Crystal Ball Collaboration, J.E. Gaiser *et al.*, Phys. Rev. D **34**, 711 (1986).
- [14] ARGUS Collaboration, H. Albrecht *et al.*, Phys. Lett. B **241**, 278 (1990).
- [15] R. Aleksan *et al.*, Phys. Lett. B **356**, 95 (1995).